Eur. Phys. J. C 22, 521–534 (2001)
Digital Object Identifier (DOI) 10.1007/s100520100819

THE EUROPEAN PHYSICAL JOURNAL C

The Higgs boson sector of the complex MSSM in the Feynman-diagrammatic approach

S. Heinemeyer[a]

HET, Brookhaven Natl. Lab., Upton, NY 11973, USA

Received: 6 August 2001 / Revised version: 8 October 2001 /
Published online: 21 November 2001 –

Abstract. In the Minimal Supersymmetric Standard Model with complex parameters (cMSSM) we calculate higher order corrections to the Higgs boson sector in the Feynman-diagrammatic approach using the on-shell renormalization scheme. The application of this approach to the cMSSM, being complementary to existing approaches, is analyzed in detail. Numerical examples for the leading fermionic corrections, including the leading two-loop effects, are presented. Numerical agreement within 10% with other approaches is found for small and moderate mixing in the scalar top sector. The leading fermionic corrections, supplemented by the full logarithmic one-loop and the leading two-loop contributions are implemented into the public Fortran code *FeynHiggsFastC*.

1 Introduction

The search for the lightest Higgs boson is a crucial test of Supersymmetry (SUSY) which can be performed with the present and the next generation of accelerators. The prediction of a relatively light Higgs boson is common to all supersymmetric models whose couplings remain in the perturbative regime up to a very high energy scale [1]. A precise prediction for the mass of the lightest Higgs boson and its couplings to other particles in terms of the relevant SUSY parameters is necessary in order to determine the discovery and exclusion potential of LEP2 and the upgraded Tevatron, and for physics at the LHC and future linear colliders, where eventually a high-precision measurement of the properties of the Higgs boson might be possible [2].

The case of the Higgs sector in the $\mathcal{CP}$-conserving MSSM has been tackled up to the two-loop level by different methods such as the Effective Potential (EP) method [3], the renormalization group (RG) improved one-loop EP approach [4] and the Feynman-diagrammatic (FD) method using the on-shell renormalization scheme [5,6]. The application of different methods lead to thorough comparisons between the different approaches. Most prominently the comparison between the RG improved one-loop EP result and the FD result [7–9], and most recently between the FD and the EP result [9,10], have been performed. These comparisons, showing agreement where expected, lead to deeper insight into the radiative corrections in the MSSM Higgs sector and thus to the confidence that the higher-order contribution, although being large, are under control.

In the case of the MSSM with complex parameters (cMSSM) the higher order corrections have yet been restricted, after the first more general investigations [11], to evaluations in the EP approach [12,13] and to the RG improved one-loop EP method [14,15]. While in the MSSM without complex parameters the FD calculation, using the on-shell renormalization scheme, has provided the only complete calculation at the one-loop level [16] and furthermore the relevant logarithmic and non-logarithmic corrections at the two-loop level [6,7], a corresponding calculation in the cMSSM has been missing so far.

This paper provides the next step into this direction: it is shown in detail how the FD method, employing the on-shell renormalization scheme, can be applied to the Higgs sector of the cMSSM. The general analysis is exemplified at the leading fermionic one-loop corrections, showing the applicability of the method and providing the full corresponding analytical result. For numerical examples and the comparison with existing approaches, the result is supplemented by non-leading corrections at the one- and two-loop level taken over from the real MSSM case. All results are finally incorporated into a public Fortran code. A detailed analysis, including a full one-loop calculation and the dominant two-loop corrections to the cMSSM Higgs sector will be presented elsewhere [17].

The rest of the paper is organized as follows. In Sect. 2 we review the Higgs sector and the scalar quark sector of the cMSSM, providing all relevant information about the relations of physical and unphysical parameters, the masses and the mixing angles. The renormalization in the on-shell scheme in the cMSSM Higgs sector is presented in detail in Sect. 3, together with the analytical result for the leading fermionic corrections obtained in this approach. Section 4 briefly reviews the evaluation of the Higgs bo-

[a] e-mail: Sven.Heinemeyer@bnl.gov

son masses and couplings in the FD approach. Numerical results for the comparison with other approaches are given in Sect. 5. Section 6 contains the description of the corresponding Fortran code *FeynHiggsFastC*. The conclusions can be found in Sect. 7.

2 Calculational basis

2.1 The tree-level Higgs sector of the cMSSM

The (c)MSSM Higgs potential reads [18]:

$$V = m_1^2 \mathcal{H}_1 \bar{\mathcal{H}}_1 + m_2^2 \mathcal{H}_2 \bar{\mathcal{H}}_2 - m_{12}^2 (\epsilon_{ab} \mathcal{H}_1^a \mathcal{H}_2^b + \text{h.c.}) + \frac{g'^2 + g^2}{8} (\mathcal{H}_1 \bar{\mathcal{H}}_1 - \mathcal{H}_2 \bar{\mathcal{H}}_2)^2 + \frac{g^2}{2} |\mathcal{H}_1 \bar{\mathcal{H}}_2|^2, \quad (1)$$

where m_1^2, m_2^2, m_{12}^2 are soft SUSY-breaking terms, g, g' are the $SU(2)$ and $U(1)$ gauge couplings, and $\epsilon_{12} = -1$. The doublet fields $\mathcal{H}_1$ and $\mathcal{H}_2$ are decomposed in the following way:

$$\mathcal{H}_1 = \begin{pmatrix} H_1^1 \\ H_1^2 \end{pmatrix} = \begin{pmatrix} v_1 + (\phi_1^0 + i\chi_1^0)/\sqrt{2} \\ \phi_1^- \end{pmatrix},$$
$$\mathcal{H}_2 = \begin{pmatrix} H_2^1 \\ H_2^2 \end{pmatrix} = e^{i\xi} \begin{pmatrix} \phi_2^+ \\ v_2 + (\phi_2^0 + i\chi_2^0)/\sqrt{2} \end{pmatrix}. \quad (2)$$

ξ is a possible new phase between the two Higgs doublets. From the unphysical parameters in (1) the transition to the physical parameters (including the tadpoles) is performed by the following substitution (see also [6,11]):

$$\begin{aligned}
v_1 &\to \frac{\sqrt{2} c_\beta s_W c_W M_Z}{e} \\
v_2 &\to \frac{\sqrt{2} s_\beta s_W c_W M_Z}{e} \\
g_1 &\to \frac{e}{c_W} \\
g_2 &\to \frac{e}{s_W} \\
m_1^2 &\to \bar{M}_{H^\pm}^2 s_\beta^2 - \frac{1}{2}(c_\beta^2 - s_\beta^2) M_Z^2 \\
&\quad + t_1 \frac{e}{2 s_W c_W M_Z} c_\beta (1 + s_\beta^2) - t_2 \frac{e}{2 s_W c_W M_Z} s_\beta c_\beta^2 \\
m_2^2 &\to \bar{M}_{H^\pm}^2 c_\beta^2 + \frac{1}{2}(c_\beta^2 - s_\beta^2) M_Z^2 - t_1 \frac{e}{2 s_W c_W M_Z} c_\beta s_\beta^2 \\
&\quad + t_2 \frac{e}{2 s_W c_W M_Z} s_\beta (1 + c_\beta^2) \\
\mathrm{Re}\, m_{12}^2 &\to \left(-\bar{M}_{H^\pm}^2 s_\beta c_\beta + t_1 \frac{e}{2 s_W c_W M_Z} s_\beta^3 \right. \\
&\quad \left. + t_2 \frac{e}{2 s_W c_W M_Z} c_\beta^3 \right) \frac{1}{\cos\xi} \\
\mathrm{Im}\, m_{12}^2 &\to \left(t_A \frac{e}{2 s_W c_W M_Z} \right) \frac{1}{\sin\xi}.
\end{aligned} \quad (3)$$

$\tan\beta$ is the ratio of the two vacuum expectation values, $\tan\beta = v_2/v_1$, and $s_\beta = \sin\beta$, $c_\beta = \cos\beta$, $c_W \equiv M_W/M_Z$, $s_W^2 = 1 - c_W^2$. $\bar{M}_{H^\pm}^2 \equiv M_{H^\pm}^2 - M_W^2$, where (as will be shown below) $M_{H^\pm}$ is the mass of the charged Higgs boson $H^\pm$. Contrary to the real case, where the mass of the $\mathcal{CP}$-odd Higgs boson, M_A, is used as input parameter, in the cMSSM $M_{H^\pm}$ is chosen as physical parameter, since the field $A \equiv s_\beta \chi_1 + c_\beta \chi_2$ (as will be shown later) mixes with the fields ϕ_1 and ϕ_2. t_1 and t_2 denote the tadpoles of the fields ϕ_1 and ϕ_2, whereas t_A is the tadpole of the field A. The expressions for the tadpoles can be obtained directly by expanding the Higgs potential (1) in the fields from the terms linear in ϕ_1, ϕ_2 and A.

In the cMSSM all neutral Higgs bosons can mix. Therefore the following (4×4) mass matrix has to be considered [11]:

$$M_{\text{Higgs}} = \begin{pmatrix} M_{\text{S}} & M_{\text{SP}} \\ M_{\text{SP}}^+ & M_{\text{P}} \end{pmatrix}, \quad (4)$$

resulting in the Lagrange density

$$\mathcal{L} = \frac{1}{2} (\phi_1, \phi_2, \chi_1, \chi_2) \quad M_{\text{Higgs}} \quad \begin{pmatrix} \phi_1 \\ \phi_2 \\ \chi_1 \\ \chi_2 \end{pmatrix}. \quad (5)$$

Here M_{S} denotes the (2×2) mass matrix of the fields ϕ_1 and ϕ_2 (the $\mathcal{CP}$-even mass matrix in the real MSSM), M_{P} represents the (2×2) mass matrix of the fields χ_1 and χ_2 (the $\mathcal{CP}$-odd mass matrix in the real MSSM). M_{SP} denotes the mixing terms (which are always zero in the real MSSM). The three matrices are given in terms of physical parameters by

$$M_{\text{S}} = \begin{pmatrix} m_{\phi_1}^2 & m_{\phi_1\phi_2}^2 \\ m_{\phi_1\phi_2}^2 & m_{\phi_2}^2 \end{pmatrix} \quad (6)$$

$$= \begin{pmatrix} \bar{M}_{H^\pm}^2 s_\beta^2 + M_Z^2 c_\beta^2 & -s_\beta c_\beta (\bar{M}_{H^\pm}^2 + M_Z^2) \\ -s_\beta c_\beta (\bar{M}_{H^\pm}^2 + M_Z^2) & \bar{M}_{H^\pm}^2 c_\beta^2 + M_Z^2 s_\beta^2 \end{pmatrix} \quad (7)$$

$$+ \begin{pmatrix} \bar{t}_1 c_\beta (1 + s_\beta^2) - \bar{t}_2 s_\beta c_\beta^2 & \bar{t}_1 s_\beta^3 + \bar{t}_2 c_\beta^3 \\ \bar{t}_1 s_\beta^3 + \bar{t}_2 c_\beta^3 & -\bar{t}_1 c_\beta s_\beta^2 + \bar{t}_2 s_\beta (1 + c_\beta^2) \end{pmatrix}$$

$$M_{\text{SP}} = \begin{pmatrix} 0 & \bar{t}_A \\ \bar{t}_A & 0 \end{pmatrix} \quad (8)$$

$$M_{\text{P}} = \begin{pmatrix} \bar{M}_{H^\pm}^2 s_\beta^2 & \bar{M}_{H^\pm}^2 s_\beta c_\beta \\ \bar{M}_{H^\pm}^2 s_\beta c_\beta & \bar{M}_{H^\pm}^2 c_\beta^2 \end{pmatrix} \quad (9)$$

$$+ \begin{pmatrix} \bar{t}_1 c_\beta (1 + s_\beta^2) - \bar{t}_2 s_\beta c_\beta^2 & -\bar{t}_1 s_\beta^3 - \bar{t}_2 c_\beta^3 \\ -\bar{t}_1 s_\beta^3 - \bar{t}_2 c_\beta^3 & -\bar{t}_1 c_\beta s_\beta^2 + \bar{t}_2 s_\beta (1 + c_\beta^2) \end{pmatrix}$$

with $\bar{t}_x \equiv t_x \, e/(2 s_W M_W)$, $x = 1, 2, A$.

Similarly the matrix of the charged Higgs bosons is given by

$$M_{\text{C}} = \begin{pmatrix} M_{H^\pm}^2 s_\beta^2 & M_{H^\pm}^2 s_\beta c_\beta \\ M_{H^\pm}^2 s_\beta c_\beta & M_{H^\pm}^2 c_\beta^2 \end{pmatrix} \quad (10)$$

$$+\begin{pmatrix} \bar{t}_1 c_\beta (1+s_\beta^2) - \bar{t}_2 s_\beta c_\beta^2 & -\bar{t}_1 s_\beta^3 - \bar{t}_2 c_\beta^3 \\ -\bar{t}_1 s_\beta^3 - \bar{t}_2 c_\beta^3 & -\bar{t}_1 c_\beta s_\beta^2 + \bar{t}_2 s_\beta (1+c_\beta^2) \end{pmatrix}$$

2.2 Rotation with β

The angle β diagonalizes (up to tadpole contributions) the matrix $M_{\rm P}$:

$$\begin{pmatrix} G \\ A \end{pmatrix} = D^+(\beta) \begin{pmatrix} \chi_1 \\ \chi_2 \end{pmatrix} = \begin{pmatrix} c_\beta & -s_\beta \\ s_\beta & c_\beta \end{pmatrix} \begin{pmatrix} \chi_1 \\ \chi_2 \end{pmatrix} \tag{11}$$

$$\begin{aligned} &(\chi_1, \chi_2)\, M_{\rm P} \begin{pmatrix} \chi_1 \\ \chi_2 \end{pmatrix} \\ &\quad = (\chi_1, \chi_2)\, D(\beta) D^+(\beta)\, M_{\rm P}\, D(\beta) D^+(\beta) \begin{pmatrix} \chi_1 \\ \chi_2 \end{pmatrix} \\ &\quad = (G, A)\, M_{\rm P}^D \begin{pmatrix} G \\ A \end{pmatrix} \end{aligned} \tag{12}$$

with

$$M_{\rm P}^D = \begin{pmatrix} c_\beta \bar{t}_1 + s_\beta \bar{t}_2 & s_\beta \bar{t}_1 - c_\beta \bar{t}_2 \\ s_\beta \bar{t}_1 - c_\beta \bar{t}_2 & \bar{M}_{H^\pm}^2 \end{pmatrix}. \tag{13}$$

This also affects the matrix $M_{\rm SP}$. Defining the (4×4) matrix

$$D^4(\beta) = \begin{pmatrix} \mathbb{1} & 0 \\ 0 & D(\beta) \end{pmatrix}, \tag{14}$$

the rotation of $M_{\rm Higgs}$ can be performed:

$$\begin{aligned} &(\phi_1, \phi_2, \chi_1, \chi_2)\, M_{\rm Higgs} \begin{pmatrix} \phi_1 \\ \phi_2 \\ \chi_1 \\ \chi_2 \end{pmatrix} \\ &\quad = (\phi_1, \phi_2, \chi_1, \chi_2)\, D^4(\beta) D^{4+}(\beta)\, M_{\rm Higgs} \\ &\qquad \times D^4(\beta) D^{4+}(\beta) \begin{pmatrix} \phi_1 \\ \phi_2 \\ \chi_1 \\ \chi_2 \end{pmatrix} \\ &\quad = (\phi_1, \phi_2, G, A)\, M_{\rm Higgs}^\beta \begin{pmatrix} \phi_1 \\ \phi_2 \\ G \\ A \end{pmatrix} \end{aligned} \tag{15}$$

with

$$M_{\rm Higgs}^\beta = \begin{pmatrix} M_{\rm S} & M_{\rm SP}^\beta \\ M_{\rm SP}^{\beta +} & M_{\rm P}^D \end{pmatrix} \tag{16}$$

and

$$M_{\rm SP}^\beta = \bar{t}_A \begin{pmatrix} -s_\beta & c_\beta \\ c_\beta & s_\beta \end{pmatrix}. \tag{17}$$

The angle β diagonalizes (up to tadpole contributions) also the matrix $M_{\rm C}$:

$$\begin{pmatrix} G^\pm \\ H^\pm \end{pmatrix} = D^+(\beta) \begin{pmatrix} \phi_1^\pm \\ \phi_2^\pm \end{pmatrix} = \begin{pmatrix} c_\beta & -s_\beta \\ s_\beta & c_\beta \end{pmatrix} \begin{pmatrix} \phi_1^\pm \\ \phi_2^\pm \end{pmatrix} \tag{18}$$

$$\begin{aligned} &(\phi_1^-, \phi_2^-)\, M_{\rm C} \begin{pmatrix} \phi_1^+ \\ \phi_2^+ \end{pmatrix} \\ &\quad = (\phi_1^-, \phi_2^-)\, D(\beta) D^+(\beta)\, M_{\rm C}\, D(\beta) D^+(\beta) \begin{pmatrix} \phi_1^+ \\ \phi_2^+ \end{pmatrix} \\ &\quad = (G^-, H^-)\, M_{\rm C}^D \begin{pmatrix} G^+ \\ H^+ \end{pmatrix} \end{aligned} \tag{19}$$

with

$$M_{\rm C}^D = \begin{pmatrix} c_\beta \bar{t}_1 + s_\beta \bar{t}_2 & +s_\beta \bar{t}_1 - c_\beta \bar{t}_2 \\ +s_\beta \bar{t}_1 - c_\beta \bar{t}_2 & M_{H^\pm}^2 \end{pmatrix}. \tag{20}$$

2.3 Rotation with α

The angle α is defined as

$$\tan 2\alpha = \tan 2\beta \frac{\bar{M}_{H^\pm}^2 + M_Z^2}{\bar{M}_{H^\pm}^2 - M_Z^2}. \tag{21}$$

It diagonalizes (up to tadpole contributions) the matrix $M_{\rm S}$ ($s_\alpha = \sin\alpha$, $c_\alpha = \cos\alpha$):

$$\begin{pmatrix} H \\ h \end{pmatrix} = D^+(\alpha) \begin{pmatrix} \phi_1 \\ \phi_2 \end{pmatrix} = \begin{pmatrix} c_\alpha & s_\alpha \\ -s_\alpha & c_\alpha \end{pmatrix} \begin{pmatrix} \phi_1 \\ \phi_2 \end{pmatrix} \tag{22}$$

$$\begin{aligned} &(\phi_1, \phi_2)\, M_{\rm S} \begin{pmatrix} \phi_1 \\ \phi_2 \end{pmatrix} \\ &\quad = (\phi_1, \phi_2) D(\alpha) D^+(\alpha)\, M_{\rm S}\, D(\alpha) D^+(\alpha) \begin{pmatrix} \phi_1 \\ \phi_2 \end{pmatrix} \\ &\quad = (H, h)\, M_{\rm S}^D \begin{pmatrix} H \\ h \end{pmatrix} \end{aligned} \tag{23}$$

with (see (24) on top of the next page) Using the (21) and setting the tadpoles to zero one obtains:

$$\begin{aligned} M_{\rm S}^D = {} & \bar{M}_{H^\pm}^2 \begin{pmatrix} (c_\beta s_\alpha - c_\alpha s_\beta)^2 & 0 \\ 0 & (c_\beta c_\alpha + s_\alpha s_\beta)^2 \end{pmatrix} \\ & + M_Z^2 \begin{pmatrix} (c_\alpha c_\beta - s_\alpha s_\beta)^2 & 0 \\ 0 & (c_\beta s_\alpha + s_\beta c_\alpha)^2 \end{pmatrix}. \end{aligned} \tag{25}$$

The rotation with α also affects the matrix $M_{\rm SP}^\beta$. Defining the (4×4) matrix

$$D^4(\alpha) = \begin{pmatrix} D(\alpha) & 0 \\ 0 & \mathbb{1} \end{pmatrix}, \tag{26}$$

$$
\begin{aligned}
M_{\rm S}^D = \; & \bar{M}^2_{H^\pm} \begin{pmatrix} (c_\beta s_\alpha - c_\alpha s_\beta)^2 & s_\beta c_\beta (s_\alpha^2 - c_\alpha^2) + s_\alpha c_\alpha (c_\beta^2 - s_\beta^2) \\ s_\beta c_\beta (s_\alpha^2 - c_\alpha^2) + s_\alpha c_\alpha (c_\beta^2 - s_\beta^2) & (c_\beta c_\alpha + s_\alpha s_\beta)^2 \end{pmatrix} \\
& + M_Z^2 \begin{pmatrix} (c_\alpha c_\beta - s_\alpha s_\beta)^2 & s_\beta c_\beta (s_\alpha^2 - c_\alpha^2) - s_\alpha c_\alpha (c_\beta^2 - s_\beta^2) \\ s_\beta c_\beta (s_\alpha^2 - c_\alpha^2) - s_\alpha c_\alpha (c_\beta^2 - s_\beta^2) & (c_\beta s_\alpha + s_\beta c_\alpha)^2 \end{pmatrix} \\
& + \bar{t}_1 \begin{pmatrix} -c_\beta s_\beta^2 s_\alpha^2 + 2 s_\alpha c_\alpha s_\beta^3 + c_\beta c_\alpha^2 (1 + s_\beta^2) & s_\beta^3 (c_\alpha^2 - s_\alpha^2) - s_\alpha c_\alpha c_\beta (1 + 2 s_\beta^2) \\ s_\beta^3 (c_\alpha^2 - s_\alpha^2) - s_\alpha c_\alpha c_\beta (1 + 2 s_\beta^2) & -2 c_\alpha s_\alpha s_\beta^3 + c_\beta (-c_\alpha^2 s_\beta^2 + s_\alpha^2 (1 + s_\beta^2)) \end{pmatrix} \\
& + \bar{t}_2 \begin{pmatrix} 2 c_\alpha s_\alpha c_\beta^3 - c_\alpha^2 c_\beta^2 s_\beta + s_\beta s_\alpha^2 (1 + c_\beta^2) & c_\beta^3 (c_\alpha^2 - s_\alpha^2) + s_\alpha c_\alpha s_\beta (1 + 2 c_\beta^2) \\ c_\beta^3 (c_\alpha^2 - s_\alpha^2) + s_\alpha c_\alpha s_\beta (1 + 2 c_\beta^2) & -2 c_\alpha s_\alpha c_\beta^3 + s_\beta (c_\alpha^2 (1 + c_\beta^2) - s_\alpha^2 c_\beta^2) \end{pmatrix}
\end{aligned} \tag{24}
$$

the rotation of $M^\beta_{\rm Higgs}$ can be performed:

$$
\begin{aligned}
& (\phi_1, \phi_2, G, A)\; M^\beta_{\rm Higgs} \begin{pmatrix} \phi_1 \\ \phi_2 \\ G \\ A \end{pmatrix} \\
& \quad = (\phi_1, \phi_2, G, A)\; D^4(\alpha) D^{4+}(\alpha)\; M^\beta_{\rm Higgs} \\
& \qquad \times D^4(\alpha) D^{4+}(\alpha) \begin{pmatrix} \phi_1 \\ \phi_2 \\ G \\ A \end{pmatrix} \\
& \quad = (H, h, G, A)\; M^D_{\rm Higgs} \begin{pmatrix} H \\ h \\ G \\ A \end{pmatrix}
\end{aligned} \tag{27}
$$

with

$$
M^D_{\rm Higgs} = \begin{pmatrix} M_{\rm S}^D & M_{\rm SP}^{\beta\alpha} \\ M_{\rm SP}^{\beta\alpha +} & M_{\rm P}^D \end{pmatrix} \tag{28}
$$

and

$$
M_{\rm SP}^{\beta\alpha} = \bar{t}_A \begin{pmatrix} -c_\alpha s_\beta + s_\alpha c_\beta & s_\alpha s_\beta + c_\alpha c_\beta \\ s_\alpha s_\beta + c_\alpha c_\beta & c_\alpha s_\beta - s_\alpha c_\beta \end{pmatrix}. \tag{29}
$$

2.4 Tree-level expressions

At tree-level all tadpoles can be set to zero. In the ϕ_1-ϕ_2 sector this ensures that $v_{1,2}$ are the vacuum expectation values. In the χ_1-χ_2 sector this corresponds to a redefinition of the phase of m_{12}^2 so that the phase $e^{i\xi}$ is absorbed [11].

One arrives at the following masses at tree-level:

$$
\begin{aligned}
H : m_H^2 = \frac{1}{2} \Bigg[& \bar{M}^2_{H^\pm} + M_Z^2 \\
& + \sqrt{(\bar{M}^2_{H^\pm} + M_Z^2)^2 - 4 M_Z^2 \bar{M}^2_{H^\pm} c^2_{2\beta}} \Bigg] \\
h : m_h^2 = \frac{1}{2} \Bigg[& \bar{M}^2_{H^\pm} + M_Z^2 \\
& - \sqrt{(\bar{M}^2_{H^\pm} + M_Z^2)^2 - 4 M_Z^2 \bar{M}^2_{H^\pm} c^2_{2\beta}} \Bigg] \\
A : M_A^2 = & M^2_{H^\pm} - M_W^2 \quad (\equiv \bar{M}^2_{H^\pm}) \\
G : m_G^2 = & M_Z^2 \\
H^\pm : M^2_{H^\pm} & \text{ (input value)} \\
G^\pm : m^2_{G^\pm} = & M_W^2
\end{aligned} \tag{30}
$$

The entries for the Goldstone bosons G and $G^\pm$ are to be understood in the Feynman gauge. At tree-level there is no $\mathcal{CP}$ violation in the cMSSM Higgs sector. The fields h and H are decoupled from the fields A and G.

2.5 The scalar quark sector in the cMSSM

The mass matrix of two squarks of the same flavor, $\tilde{q}_L$ and $\tilde{q}_R$, is given by

$$
M_{\tilde{q}} = \begin{pmatrix} M_L^2 + m_q^2 & m_q\, X_q^* \\ m_q\, X_q & M_R^2 + m_q^2 \end{pmatrix} \tag{31}
$$

with

$$
\begin{aligned}
M_L^2 &= M_{\tilde{Q}}^2 + M_Z^2 \cos 2\beta\; (I_3^q - Q_q s_W^2) \\
M_R^2 &= M_{\tilde{Q}'}^2 + M_Z^2 \cos 2\beta\; Q_q s_W^2 \\
X_q &= A_q - \mu^* \{\cot\beta\,, \tan\beta\},
\end{aligned} \tag{32}
$$

where $\{\cot\beta\,, \tan\beta\}$ applies for $\{\text{up}, \text{down}\}$-type squarks respectively. In an isodoublet the $SU(2)$ symmetry enforces that $M_{\tilde{Q}}$ has to be chosen equal for both squark types. The $M_{\tilde{Q}'}$ on the other hand can be chosen independently for every squark type. In the scalar quark sector of the cMSSM $N_q + 1$ phases are present, one for each A_q and one for μ, i.e. $N_q + 1$ new parameters appear. As an abbreviation it will be used

$$
\phi_q = \arg(X_q)\,. \tag{33}
$$

As an independent parameter one can trade $\arg(A_q) \equiv \phi_{A_q}$ for ϕ_q.

The squark mass eigenstates are obtained by the rotation

$$\begin{pmatrix} \tilde{q}_1 \\ \tilde{q}_2 \end{pmatrix} = S^{\tilde{q}} \begin{pmatrix} \tilde{q}_L \\ \tilde{q}_R \end{pmatrix} \tag{34}$$

with

$$S^{\tilde{q}} = \begin{pmatrix} c_{\tilde{q}} & s^*_{\tilde{q}} \\ -s_{\tilde{q}} & c^*_{\tilde{q}} \end{pmatrix} = \begin{pmatrix} e^{i\phi_q/2}|c_{\tilde{q}}| & e^{-i\phi_q/2}|s_{\tilde{q}}| \\ -e^{i\phi_q/2}|s_{\tilde{q}}| & e^{-i\phi_q/2}|c_{\tilde{q}}| \end{pmatrix},$$
$$S^{\tilde{q}+} S^{\tilde{q}} = \mathbb{1}\,, \tag{35}$$

where the matrix with $\phi_q \to 0$ diagonalizes $M_{\tilde{q}}\Big|_{X_q \to |X_q|}$.

The mass eigenvalues are given by

$$m^2_{\tilde{q}_{1,2}} = m^2_q + \frac{1}{2}\Bigg[M^2_L + M^2_R \mp \sqrt{(M^2_L - M^2_R)^2 + 4m^2_q |X_q|^2}\Bigg], \tag{36}$$

independent of the phase of X_q. The unrotated squark mass matrix can now be expressed in terms of the physical parameters $m_{\tilde{q}_1}, m_{\tilde{q}_2}$ and the $\tilde{q}$ mixing angle:

$$M_{\tilde{q}} = \begin{pmatrix} c_{\tilde{q}} c^*_{\tilde{q}} m^2_{\tilde{q}_1} + s_{\tilde{q}} s^*_{\tilde{q}} m^2_{\tilde{q}_2} & s^*_{\tilde{q}} c^*_{\tilde{q}} (m^2_{\tilde{q}_1} - m^2_{\tilde{q}_2}) \\ s_{\tilde{q}} c_{\tilde{q}} (m^2_{\tilde{q}_1} - m^2_{\tilde{q}_2}) & s_{\tilde{q}} s^*_{\tilde{q}} m^2_{\tilde{q}_1} + c_{\tilde{q}} c^*_{\tilde{q}} m^2_{\tilde{q}_2} \end{pmatrix}. \tag{37}$$

3 Calculation of the renormalized self-energies

3.1 Renormalization

The renormalization is performed as follows:

$$\begin{aligned} M^2_{H^\pm} &\to M^2_{H^\pm} + \delta M^2_{H^\pm} \\ M^2_W &\to M^2_W + \delta M^2_W \\ M^2_Z &\to M^2_Z + \delta M^2_Z \\ t_x &\to t_x + \delta t_x, \quad x = 1,2,A \\ \tan\beta &\to \tan\beta + \delta\tan\beta \\ \mathcal{H}_1 &\to Z^{1/2}_{H_1} \mathcal{H}_1 \\ \mathcal{H}_2 &\to Z^{1/2}_{H_2} \mathcal{H}_2 \end{aligned} \tag{38}$$

The counterterm for the A tadpole can be understood as the effect of re normalizing the phase ξ of $\mathcal{H}_2$.

In the following we will concentrate on the contributions that are relevant for the leading m_t^4 corrections (or any corrections of the type $\sim m_f^4$) for the masses of the neutral Higgs bosons. There, only $\delta M^2_{H^\pm}$ and $\delta t_x, x = 1,2,A$, enter (see also [6]).

The renormalized $H^\pm$ self-energy is then given by

$$\mathrm{Re}\,\hat{\Sigma}_{H^\pm}(0) = \Sigma_{H^\pm}(0) - \delta M^2_{H^\pm}, \tag{39}$$

the renormalized tadpoles are given by

$$\hat{t}_x = T_x + \delta t_x, \quad x = 1,2,A, \tag{40}$$

T_x represents the one-loop contribution to t_x.

The on-shell renormalization conditions are imposed:

$$\mathrm{Re}\,\hat{\Sigma}_{H^\pm}(0) = 0\,, \tag{41}$$
$$\hat{t}_x = 0\,. \tag{42}$$

This results in the on-shell renormalization constants

$$\delta M^2_{H^\pm} = \Sigma_{H^\pm}(0)\,, \tag{43}$$
$$\delta t_x = -T_x\,. \tag{44}$$

Since the charged Higgs boson is renormalized on-shell, its mass does not receive higher-order corrections.

3.2 Renormalized self-energies

With the on-shell renormalization constants derived in Sect. 3.1 the renormalized neutral Higgs boson self-energies read:

$$\begin{aligned} \hat{\Sigma}_{hh}(0) &= \Sigma_{hh}(0) - \delta M^2_{H^\pm}(c_\alpha c_\beta + s_\alpha s_\beta)^2 + T_1 \frac{e}{2 s_W M_W} \\ &\quad \times(-2c_\alpha s_\alpha s^3_\beta + c_\beta(-c^2_\alpha s^2_\beta + s^2_\alpha(1+s^2_\beta))) \\ &\quad + T_2 \frac{e}{2 s_W M_W} \\ &\quad \times(-2c_\alpha s_\alpha c^3_\beta + s_\beta(c^2_\alpha(1+c^2_\beta) - s^2_\alpha c^2_\beta)) \end{aligned} \tag{45}$$

$$\begin{aligned} \hat{\Sigma}_{HH}(0) &= \Sigma_{HH}(0) - \delta M^2_{H^\pm}(s_\alpha c_\beta - c_\alpha s_\beta)^2 \\ &\quad + T_1 \frac{e}{2 s_W M_W} \\ &\quad \times(-c_\beta s^2_\alpha s^2_\beta + 2 s_\alpha c_\alpha s^3_\beta + c^2_\alpha c_\beta(1+s^2_\beta)) \\ &\quad + T_2 \frac{e}{2 s_W M_W} \\ &\quad \times(2 s_\alpha c_\alpha c^3_\beta - c^2_\alpha c^2_\beta s_\beta + (1+c^2_\beta) s^2_\alpha s_\beta) \end{aligned} \tag{46}$$

$$\begin{aligned} \hat{\Sigma}_{hH}(0) &= \Sigma_{hH}(0) - \delta M^2_{H^\pm} \\ &\quad \times(s_\beta c_\beta(s^2_\alpha - c^2_\alpha) + s_\alpha c_\alpha(c^2_\beta - s^2_\beta)) \\ &\quad + T_1 \frac{e}{2 s_W M_W}(s^3_\beta(c^2_\alpha - s^2_\alpha) - s_\alpha c_\alpha c_\beta(1+2s^2_\beta)) \\ &\quad + T_2 \frac{e}{2 s_W M_W} \\ &\quad \times(c^3_\beta(c^2_\alpha - s^2_\alpha) + s_\alpha c_\alpha s_\beta(1+2c^2_\beta)) \end{aligned} \tag{47}$$

$$\hat{\Sigma}_{AA}(0) = \Sigma_{AA}(0) - \delta M^2_{H^\pm} \tag{48}$$

$$\hat{\Sigma}_{GG}(0) = \Sigma_{GG}(0) + \frac{e}{2 s_W M_W}(-T_1 c_\beta - T_2 s_\beta) \tag{49}$$

$$\hat{\Sigma}_{AG}(0) = \Sigma_{AG}(0) + \frac{e}{2 s_W M_W}(-T_1 s_\beta + T_2 c_\beta) \tag{50}$$

$$\hat{\Sigma}_{hA}(0) = \Sigma_{hA}(0) + T_A \frac{e}{2 s_W M_W}(-c_\alpha s_\beta + s_\alpha c_\beta) \tag{51}$$

$$\hat{\Sigma}_{HA}(0) = \Sigma_{HA}(0) + T_A \frac{e}{2 s_W M_W}(-s_\alpha s_\beta - c_\alpha c_\beta) \tag{52}$$

$$\hat{\Sigma}_{hG}(0) = \Sigma_{hG}(0) + T_A \frac{e}{2 s_W M_W}(-s_\alpha s_\beta - c_\alpha c_\beta) \tag{53}$$

$$\hat{\Sigma}_{HG}(0) = \Sigma_{HG}(0) + T_A \frac{e}{2 s_W M_W}(-s_\alpha c_\beta + c_\alpha s_\beta) \tag{54}$$

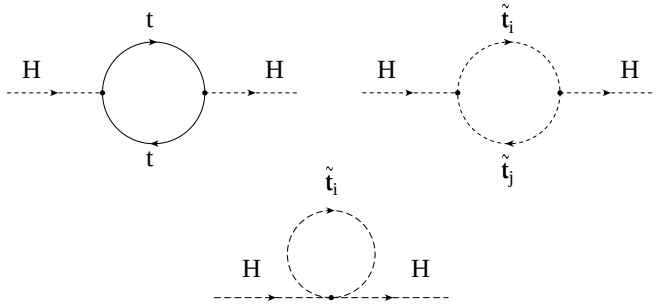

Fig. 1. Generic Feynman diagrams for the m_t^4 contributions to Higgs self-energies

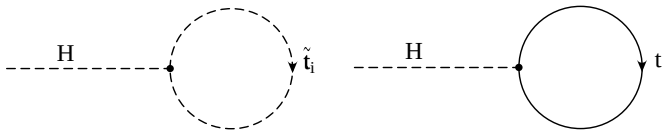

Fig. 2. Generic Feynman diagrams for the m_t^4 contributions to Higgs tadpoles

3.3 Evaluation of m_t^4 contributions

For the evaluation of the leading m_t^4 corrections in the Feynman-diagrammatic (FD) approach the diagrams shown in Fig. 1 have to be evaluated for all self-energies $\Sigma_{st}(0), st = hh, HH, hH, AA, GG, AG, hA, HA, hG, HG$. Concerning the tadpole contributions the diagrams of Fig. 2 have to be considered.

For sake of simplicity we now switch back to the ϕ_1-ϕ_2 basis (i.e. $\alpha = 0$), where the results have a much simpler form. The corresponding results in the h-H basis can be obtained by the rotation

$$
\begin{aligned}
\hat{\Sigma}_{hh} &= \sin^2\alpha\ \hat{\Sigma}_{\phi_1} + \cos^2\alpha\ \hat{\Sigma}_{\phi_2} - 2\sin\alpha\ \cos\alpha\ \hat{\Sigma}_{\phi_1\phi_2} \\
\hat{\Sigma}_{HH} &= \cos^2\alpha\ \hat{\Sigma}_{\phi_1} + \sin^2\alpha\ \hat{\Sigma}_{\phi_2} + 2\sin\alpha\ \cos\alpha\ \hat{\Sigma}_{\phi_1\phi_2} \\
\hat{\Sigma}_{hH} &= -\sin\alpha\ \cos\alpha\ \left(\hat{\Sigma}_{\phi_1} - \hat{\Sigma}_{\phi_2}\right) \\
&\quad +(\cos^2\alpha\ - \sin^2\alpha\ )\hat{\Sigma}_{\phi_1\phi_2} \\
\hat{\Sigma}_{hA} &= -\sin\alpha\ \hat{\Sigma}_{\phi_1 A} + \cos\alpha\ \hat{\Sigma}_{\phi_2 A} \\
\hat{\Sigma}_{HA} &= \cos\alpha\ \hat{\Sigma}_{\phi_1 A} + \sin\alpha\ \hat{\Sigma}_{\phi_2 A} \\
\hat{\Sigma}_{hG} &= -\sin\alpha\ \hat{\Sigma}_{\phi_1 G} + \cos\alpha\ \hat{\Sigma}_{\phi_2 G} \\
\hat{\Sigma}_{HG} &= \cos\alpha\ \hat{\Sigma}_{\phi_1 G} + \sin\alpha\ \hat{\Sigma}_{\phi_2 G}.
\end{aligned} \tag{55}
$$

The m_t^4 corrections have been obtained using the program *FeynArts* 3 [19], employing the recently completed MSSM model file [20][1]. Details about the calculations with *FeynArts* can be found in [21]. In the approximation of the leading m_t^4 corrections (and with $m_b = 0$) the result for the renormalized self-energies of (45) - (54) reads:

$$
\begin{aligned}
&\hat{\Sigma}_{\phi_1\phi_1}(0) \\
&= \frac{3\,e^2 M_Z^2}{32(M_W^2 - M_Z^2)\pi^2 s_\beta^2}\frac{m_t^2}{M_W^2} \\
&\quad\times\Big\{(s_{\tilde{t}}^2 c_{\tilde{t}}^2\mu^2 + s_{\tilde{t}}^{*2} c_{\tilde{t}}^{*2}\mu^{*2})\, g(m_{\tilde{t}_1}, m_{\tilde{t}_2}) \\
&\quad -\Delta_{H^\pm A} s_\beta^2\Big\}
\end{aligned} \tag{56}
$$

$$
\begin{aligned}
&\hat{\Sigma}_{\phi_2\phi_2}(0) \\
&= \frac{3\,e^2 M_Z^2}{32(M_W^2 - M_Z^2)\pi^2 s_\beta^2}\frac{m_t^2}{M_W^2} \\
&\quad\times\Bigg\{ -\Delta_{H^\pm A} c_\beta^2\ - 2m_t^2 \log\left(\frac{m_t^4}{m_{\tilde{t}_1}^2 m_{\tilde{t}_2}^2}\right) \\
&\quad +\Bigg[\frac{c_\beta^2}{s_\beta^2}(s_{\tilde{t}}^2 c_{\tilde{t}}^2\mu^2 + s_{\tilde{t}}^{*2} c_{\tilde{t}}^{*2}\mu^{*2}) + 2\frac{c_\beta}{s_\beta}\frac{m_{\tilde{t}_1}^2 - m_{\tilde{t}_2}^2}{m_t} \\
&\quad\times(s_{\tilde{t}} c_{\tilde{t}}\mu + s_{\tilde{t}}^* c_{\tilde{t}}^*\mu^*) s_{\tilde{t}} s_{\tilde{t}}^* c_{\tilde{t}} c_{\tilde{t}}^* \\
&\quad +2 s_{\tilde{t}}^2 s_{\tilde{t}}^{*2} c_{\tilde{t}}^2 c_{\tilde{t}}^{*2}\frac{(m_{\tilde{t}_1}^2 - m_{\tilde{t}_2}^2)^2}{m_t^2}\Bigg] g(m_{\tilde{t}_1}, m_{\tilde{t}_2}) \\
&\quad +\Bigg[2m_t\frac{c_\beta}{s_\beta}(s_{\tilde{t}} c_{\tilde{t}}\mu + s_{\tilde{t}}^* c_{\tilde{t}}^*\mu^*) \\
&\quad +4 s_{\tilde{t}} s_{\tilde{t}}^* c_{\tilde{t}} c_{\tilde{t}}^*(m_{\tilde{t}_1}^2 - m_{\tilde{t}_2}^2)\Bigg] \log\left(\frac{m_{\tilde{t}_1}^2}{m_{\tilde{t}_2}^2}\right)\Bigg\}
\end{aligned} \tag{57}
$$

$$
\begin{aligned}
&\hat{\Sigma}_{\phi_1\phi_2}(0) \\
&= -\frac{3\,e^2 M_Z^2}{32(M_W^2 - M_Z^2)\pi^2 s_\beta^2}\frac{m_t^2}{M_W^2}\Bigg\{ -\Delta_{H^\pm A} s_\beta c_\beta \\
&\quad +\Bigg[\frac{c_\beta}{s_\beta}(s_{\tilde{t}}^2 c_{\tilde{t}}^2\mu^2 + s_{\tilde{t}}^{*2} c_{\tilde{t}}^{*2}\mu^{*2}) \\
&\quad +(s_{\tilde{t}} c_{\tilde{t}}\mu + s_{\tilde{t}}^* c_{\tilde{t}}^*\mu^*) s_{\tilde{t}} s_{\tilde{t}}^* c_{\tilde{t}} c_{\tilde{t}}^*\frac{m_{\tilde{t}_1}^2 - m_{\tilde{t}_2}^2}{m_t}\Bigg] g(m_{\tilde{t}_1}, m_{\tilde{t}_2}) \\
&\quad +(s_{\tilde{t}} c_{\tilde{t}}\mu + s_{\tilde{t}}^* c_{\tilde{t}}^*\mu^*) m_t \log\left(\frac{m_{\tilde{t}_1}^2}{m_{\tilde{t}_2}^2}\right)\Bigg\}
\end{aligned} \tag{58}
$$

$$
\begin{aligned}
&\hat{\Sigma}_{AA}(0) \\
&= -\frac{3\,e^2 M_Z^2}{32(M_W^2 - M_Z^2)\pi^2 s_\beta^2}\frac{m_t^2}{M_W^2}\ \Delta_{H^\pm A} \\
&\quad (\equiv \Sigma_{AA}(0) - \Sigma_{H^\pm}(0))
\end{aligned} \tag{59}
$$

$$\hat{\Sigma}_{H^\pm}(0) = 0 \quad \text{(by renormalization)} \tag{60}$$

$$\hat{\Sigma}_{GG}(0) = 0 \tag{61}$$

$$\hat{\Sigma}_{AG}(0) = 0 \tag{62}$$

$$
\begin{aligned}
&\hat{\Sigma}_{\phi_1 A}(0) \\
&= \frac{3i\,e^2 M_Z^2}{64(M_W^2 - M_Z^2)\pi^2 s_\beta^3}\frac{m_t^2}{M_W^2} \\
&\quad\times(s_{\tilde{t}}^2 c_{\tilde{t}}^2\mu^2 - s_{\tilde{t}}^{*2} c_{\tilde{t}}^{*2}\mu^{*2})\, g(m_{\tilde{t}_1}, m_{\tilde{t}_2})
\end{aligned} \tag{63}
$$

$$
\begin{aligned}
&\hat{\Sigma}_{\phi_2 A}(0) \\
&= -\frac{3i\,e^2 M_Z^2}{64(M_W^2 - M_Z^2)\pi^2 s_\beta^3}\frac{m_t^2}{M_W^2} \\
&\quad\times\Bigg\{\Bigg[\frac{c_\beta}{s_\beta}(s_{\tilde{t}}^2 c_{\tilde{t}}^2\mu^2 - s_{\tilde{t}}^{*2} c_{\tilde{t}}^{*2}\mu^{*2}) + 2\frac{m_{\tilde{t}_1}^2 - m_{\tilde{t}_2}^2}{m_t}
\end{aligned}
$$

[1] Only the non-SM counterterms had to be added.

$$\times(s_{\tilde{t}}c_{\tilde{t}}\mu - s^*_{\tilde{t}}c^*_{\tilde{t}}\mu^*)s_{\tilde{t}}s^*_{\tilde{t}}c_{\tilde{t}}c^*_{\tilde{t}}\Bigg] g(m_{\tilde{t}_1}, m_{\tilde{t}_2})$$
$$+2m_t(s_{\tilde{t}}c_{\tilde{t}}\mu - s^*_{\tilde{t}}c^*_{\tilde{t}}\mu^*)\log\left(\frac{m^2_{\tilde{t}_1}}{m^2_{\tilde{t}_2}}\right)\Bigg\} \quad (64)$$

$$\hat{\Sigma}_{\phi_1 G}(0) = 0 \quad (65)$$

$$\hat{\Sigma}_{\phi_2 G}(0) = 0 \quad (66)$$

with

$$g(x,y) = 2 - \frac{x^2+y^2}{x^2-y^2}\log\left(\frac{x^2}{y^2}\right)$$

$$\Delta_{H^\pm A} \equiv \frac{1}{s^2_\beta}\left[s^2_{\tilde{t}}c^2_{\tilde{t}}\mu^2 - 2s_{\tilde{t}}s^*_{\tilde{t}}c_{\tilde{t}}c^*_{\tilde{t}}\mu\mu^* + s^{*2}_{\tilde{t}}c^{*2}_{\tilde{t}}\mu^{*2}\right]$$
$$-\frac{m^2_{\tilde{b}_L}m^2_t\mu\mu^*}{2s^2_\beta(m^2_{\tilde{b}_L}-m^2_{\tilde{t}_1})(m^2_{\tilde{b}_L}-m^2_{\tilde{t}_2})}$$
$$\times\log\left(\frac{m^4_{\tilde{b}_L}}{m^2_{\tilde{t}_1}m^2_{\tilde{t}_2}}\right) + \frac{1}{2s^2_\beta}\log\left(\frac{m^2_{\tilde{t}_1}}{m^2_{\tilde{t}_2}}\right)$$
$$\times\Bigg\{-\frac{m^2_{\tilde{t}_1}+m^2_{\tilde{t}_2}}{m^2_{\tilde{t}_1}-m^2_{\tilde{t}_2}}\left(s^2_{\tilde{t}}c^2_{\tilde{t}}\mu^2 + s^{*2}_{\tilde{t}}c^{*2}_{\tilde{t}}\mu^{*2}\right)$$
$$+\mu\mu^*\Bigg[2(s_{\tilde{t}}s^*_{\tilde{t}} - c_{\tilde{t}}c^*_{\tilde{t}}) - \frac{2}{m^2_{\tilde{t}_1}-m^2_{\tilde{t}_2}}$$
$$\times\left(s^2_{\tilde{t}}s^{*2}_{\tilde{t}}m^2_{\tilde{t}_1} + c^2_{\tilde{t}}c^{*2}_{\tilde{t}}m^2_{\tilde{t}_2}\right)$$
$$+m^2_{\tilde{b}_L}\left(\frac{c_{\tilde{t}}c^*_{\tilde{t}}}{m^2_{\tilde{b}_L}-m^2_{\tilde{t}_2}} - \frac{s_{\tilde{t}}s^*_{\tilde{t}}}{m^2_{\tilde{b}_L}-m^2_{\tilde{t}_1}}\right)\Bigg]\Bigg\} \quad (67)$$

$$m^2_{\tilde{b}_L} \equiv c_{\tilde{t}}c^*_{\tilde{t}}m^2_{\tilde{t}_1} + s_{\tilde{t}}s^*_{\tilde{t}}m^2_{\tilde{t}_2} - m^2_t \quad (68)$$

As expected, $\hat{\Sigma}_{hG}(0) = \hat{\Sigma}_{HG}(0) = \hat{\Sigma}_{AG}(0) = \hat{\Sigma}_{GG}(0) = 0$, i.e. the Goldstone boson G decouples [11]. In order to show the finiteness of $\hat{\Sigma}_{st}$, $st = \phi_1\phi_1, \phi_2\phi_2, \phi_1\phi_2, AA, \phi_1 A, \phi_2 A$ it was necessary to employ the $SU(2)$ symmetry in the scalar quark sector, see Sect. 2.5. In the simplified case of the leading m_t^4 corrections and $m_b = 0$ (i.e. no mixing in the $\tilde{b}$ sector) only the left-handed scalar bottom quark, $\tilde{b}_L$ contributes, where its mass is given by (68).

Exactly analogous expressions have been obtained for the leading m_b^4 corrections (with $m_{\tilde{t}} \leftrightarrow m_{\tilde{b}}$ and $s_\beta \leftrightarrow c_\beta$ (except in the $\Delta_{H^\pm A}$ prefactor)), which can be relevant for large $\tan\beta$. Analogous to the m_b^4 corrections also the corresponding m_τ^4 contributions (up to the color factor and with $m_{\tilde{b}} \to m_{\tilde{\tau}}$) have been evaluated.

A main difference compared to the RG improved EP approach as presented in [14] is the validity of the result as a function of the $\tilde{t}$ sector parameters. Since the FD result is obtained directly in terms of the physical parameters in the squark sector, the results of the FD approach are valid for arbitrary mixing in the $\tilde{t}$ sector, whereas the RG method is restricted to $(m^2_{\tilde{t}_2} - m^2_{\tilde{t}_1})/(m^2_{\tilde{t}_2} + m^2_{\tilde{t}_1}) \lesssim 1/2$.

3.4 Corrections beyond one-loop order

Since it is known in the case of vanishing complex phases that the two-loop corrections to the neutral Higgs boson masses can be large, for the further numerical examples and comparisons as presented in Sect. 5, the leading contributions at $\mathcal{O}(G_F\alpha_s m_t^4)$ and $\mathcal{O}(G_F^2 m_t^6)$ are taken into account. For sake of simplicity, up to now the two-loop corrections are taken over from the $\mathcal{CP}$-conserving case. The leading corrections then only affect $\hat{\Sigma}_{\phi_2\phi_2}(0)$ and are valid for arbitrary Higgs sector parameters. They are given by [4,22,23]

$$\hat{\Sigma}^{2,\alpha\alpha_s}_{\phi_2\phi_2}(0) = \frac{G_F\sqrt{2}}{\pi^2}\frac{\alpha_s}{\pi}\frac{\overline{m}_t^4}{\sin^2\beta}\Bigg[4 + 3\log^2\left(\frac{\overline{m}_t^2}{M_S^2}\right)$$
$$+2\log\left(\frac{\overline{m}_t^2}{M_S^2}\right) - 6\frac{X_t}{M_S}$$
$$-\frac{X_t^2}{M_S^2}\left\{3\log\left(\frac{\overline{m}_t^2}{M_S^2}\right) + 8\right\} + \frac{17}{12}\frac{X_t^4}{M_S^4}\Bigg] \quad (69)$$

$$\hat{\Sigma}^{2,\alpha^2}_{\phi_2\phi_2}(0) = -\frac{9}{16\pi^4}G_F^2\frac{\overline{m}_t^6}{\sin^2\beta}\left[\tilde{X}t + t^2\right], \quad (70)$$

$$\tilde{X} = \Bigg[\left(\frac{m^2_{\tilde{t}_2} - m^2_{\tilde{t}_1}}{4\overline{m}_t^2}\sin^2 2\theta_{\tilde{t}}\right)^2$$
$$\times\left(2 - \frac{m^2_{\tilde{t}_2}+m^2_{\tilde{t}_1}}{m^2_{\tilde{t}_2}-m^2_{\tilde{t}_1}}\log\left(\frac{m^2_{\tilde{t}_2}}{m^2_{\tilde{t}_1}}\right)\right)$$
$$+\frac{m^2_{\tilde{t}_2}-m^2_{\tilde{t}_1}}{2\overline{m}_t^2}\sin^2 2\theta_{\tilde{t}}\log\left(\frac{m^2_{\tilde{t}_2}}{m^2_{\tilde{t}_1}}\right)\Bigg],$$

$$t = \frac{1}{2}\log\left(\frac{m^2_{\tilde{t}_1}m^2_{\tilde{t}_2}}{\overline{m}_t^4}\right).$$

M_S has to be chosen according to

$$M_S = \begin{cases} \sqrt{m_{\tilde{q}}^2 + m_t^2} \\ \quad : M_{\tilde{t}_L} = M_{\tilde{t}_R} = m_{\tilde{q}} \\ \left[M^2_{\tilde{t}_L}M^2_{\tilde{t}_R} + m_t^2(M^2_{\tilde{t}_L} + M^2_{\tilde{t}_R}) + m_t^4\right]^{\frac{1}{4}} \\ \quad : M_{\tilde{t}_L} \neq M_{\tilde{t}_R} \end{cases} \quad (71)$$

and $\overline{m}_t$ denotes the running top quark mass, $\overline{m}_t = \overline{m}_t(m_t)$. $M_{\tilde{t}_L}, M_{\tilde{t}_R}$ correspond to $M_{\tilde{Q}}, M_{\tilde{Q}'}$ in (33) respectively. Contrary to the presented one-loop result for $\hat{\Sigma}_{\phi_2\phi_2}$, (69) is valid only for not too large mass splitting between the two $\tilde{t}$ mass eigenstates, but still gives a rather good approximation for a large part of the MSSM parameter space [22]. The full result in [17], however, will be obtained in terms of the physical parameters and thus be valid for arbitrary mixing in the $\tilde{t}$ sector. Also (70) is valid for not too large mass splitting in the $\tilde{t}$ sector [4, 23]. However, since the numerical effect of the correction in (70) is at the $\sim 2\,\text{GeV}$ level [6], this additional uncertainty is neglected. Furthermore, (70) has been obtained in the $\overline{\text{MS}}$ scheme, while all other corrections in this paper

$$M_{\mathcal{CP}} = \begin{pmatrix} M_{11} & M_{12} & M_{13} \\ M_{21} & M_{22} & M_{23} \\ M_{31} & M_{32} & M_{33} \end{pmatrix} = \begin{pmatrix} \bar{M}^2_{H^\pm} - \hat{\Sigma}_{AA}(0) & -\hat{\Sigma}_{\phi_1 A}(0) & -\hat{\Sigma}_{\phi_2 A}(0) \\ -\hat{\Sigma}_{\phi_1 A}(0) & m^2_{\phi_1} - \hat{\Sigma}_{\phi_1\phi_1}(0) & m^2_{\phi_1\phi_2} - \hat{\Sigma}_{\phi_1\phi_2}(0) \\ -\hat{\Sigma}_{\phi_2 A}(0) & m^2_{\phi_1\phi_2} - \hat{\Sigma}_{\phi_1\phi_2}(0) & m^2_{\phi_2} - \hat{\Sigma}_{\phi_2\phi_2}(0) \end{pmatrix}. \tag{72}$$

are evaluated in the on-shell scheme. The corresponding uncertainty is only of $\mathcal{O}(\alpha^2\alpha_s)$ and expected to be below $\sim 1\,\text{GeV}$ and therefore neglected.

4 The neutral MSSM Higgs sector

4.1 The Higgs boson masses

In this section, for sake of completeness, we review the derivation of the Higgs boson masses from the calculated higher-order Higgs boson self-energies. Since in the approximation used in Sect. 3.3 the external momentum has been set to zero, this step of the evaluation is equal to the EP approach [12–14]. In the full FD calculation [17] the momentum dependence, however, is included, which can lead to corrections of $1 - 2\,\text{GeV}$.

Since the Goldstone boson G decouples, see Sect. 3.3, the fields ϕ_1, ϕ_2 and A form a closed subspace that can be evaluated on its own. The masses at higher order can be obtained from the diagonalization of the matrix (see (72) on top of the page) The diagonalization is performed with the help of the (3×3) orthogonal matrix D^3:

$$\begin{aligned} &(A, \phi_1, \phi_2)\ M_{\mathcal{CP}} \begin{pmatrix} A \\ \phi_1 \\ \phi_2 \end{pmatrix} \\ &\quad = (A, \phi_1, \phi_2)\ D^3 D^{3+}\ M_{\mathcal{CP}}\ D^3 D^{3+} \begin{pmatrix} A \\ \phi_1 \\ \phi_2 \end{pmatrix} \\ &\quad = (H_3, H_2, H_1)\ M^D_{\mathcal{CP}} \begin{pmatrix} H_3 \\ H_2 \\ H_1 \end{pmatrix} \end{aligned} \tag{73}$$

with

$$M^D_{\mathcal{CP}} = \begin{pmatrix} m^2_{H_3} & 0 & 0 \\ 0 & m^2_{H_2} & 0 \\ 0 & 0 & m^2_{H_1} \end{pmatrix}, \quad m_{H_3} \geq m_{H_2} \geq m_{H_1}. \tag{74}$$

The numerical evaluation of $M^D_{\mathcal{CP}}$ and D^3 has been presented e.g. in [14] and is also listed here for completeness. The eigenvalues of $M_{\mathcal{CP}}$ are given by

$$\begin{aligned} e_1 &= -\frac{1}{3}r + 2\sqrt{-p/3}\,\cos\left(\frac{\varphi}{3}\right), \\ e_2 &= -\frac{1}{3}r + 2\sqrt{-p/3}\,\cos\left(\frac{\varphi}{3} + \frac{2\pi}{3}\right), \\ e_3 &= -\frac{1}{3}r + 2\sqrt{-p/3}\,\cos\left(\frac{\varphi}{3} - \frac{2\pi}{3}\right), \end{aligned} \tag{75}$$

with

$$\begin{aligned} p &= \frac{3s - r^2}{3}, \quad q = \frac{2r^3}{27} - \frac{rs}{3} + t, \\ \varphi &= \arccos\left(-\frac{q}{2\sqrt{-p^3/27}}\right) \end{aligned} \tag{76}$$

and

$$\begin{aligned} r &= -\text{Tr}\left(M_{\mathcal{CP}}\right), \quad s = \frac{1}{2}\left[\text{Tr}^2\left(M_{\mathcal{CP}}\right) - \text{Tr}\left(M^2_{\mathcal{CP}}\right)\right], \\ t &= -\text{Det}\left(M_{\mathcal{CP}}\right). \end{aligned} \tag{77}$$

The rotation matrix D^3 can be obtained as

$$\begin{aligned} D^3 &= \begin{pmatrix} |x_1|/\Delta_1 & x_2/\Delta_2 & x_3/\Delta_3 \\ y_1/\Delta_1 & |y_2|/\Delta_2 & y_3/\Delta_3 \\ z_1/\Delta_1 & z_2/\Delta_2 & |z_3|/\Delta_3 \end{pmatrix}, \\ \Delta_i &= \sqrt{x_i^2 + y_i^2 + z_i^2}, \end{aligned} \tag{78}$$

where

$$\begin{aligned} x_1 &= \text{Det}\begin{pmatrix} M_{22} - m^2_{H_3} & M_{23} \\ M_{32} & M_{33} - m^2_{H_3} \end{pmatrix} \\ y_2 &= \text{Det}\begin{pmatrix} M_{11} - m^2_{H_2} & M_{13} \\ M_{31} & M_{33} - m^2_{H_2} \end{pmatrix} \\ z_3 &= \text{Det}\begin{pmatrix} M_{11} - m^2_{H_1} & M_{12} \\ M_{21} & M_{22} - m^2_{H_1} \end{pmatrix} \\ x_2 &= \text{Det}\begin{pmatrix} M_{13} & M_{12} \\ M_{33} - m^2_{H_2} & M_{32} \end{pmatrix} \times \text{sign}(y_2) \\ x_3 &= \text{Det}\begin{pmatrix} M_{12} & M_{13} \\ M_{22} - m^2_{H_1} & M_{23} \end{pmatrix} \times \text{sign}(z_3) \\ y_1 &= \text{Det}\begin{pmatrix} M_{23} & M_{21} \\ M_{33} - m^2_{H_3} & M_{31} \end{pmatrix} \times \text{sign}(x_1) \\ y_3 &= \text{Det}\begin{pmatrix} M_{13} & M_{11} - m^2_{H_1} \\ M_{23} & M_{21} \end{pmatrix} \times \text{sign}(z_3) \\ z_1 &= \text{Det}\begin{pmatrix} M_{21} & M_{22} - m^2_{H_3} \\ M_{31} & M_{32} \end{pmatrix} \times \text{sign}(x_1) \\ z_2 &= \text{Det}\begin{pmatrix} M_{12} & M_{11} - m^2_{H_2} \\ M_{32} & M_{31} \end{pmatrix} \times \text{sign}(y_2) \end{aligned} \tag{79}$$

4.2 The Higgs boson couplings

Again we follow the prescriptions as given in [14]. Taking complex phases into account, all three neutral Higgs

bosons are composed of a $\mathcal{CP}$-even part, thus all three Higgs bosons can couple to two gauge boson, $VV = ZZ$, W^+W^-. The coupling normalized to the SM value is given by

$$g_{H_iVV} = c_\beta D^3_{2,4-i} + s_\beta D^3_{3,4-i} \quad . \tag{80}$$

The coupling of two Higgs bosons to a Z boson, normalized to the SM value, is given by

$$\begin{aligned} g_{H_iH_jZ} = {} & D^3_{1,4-i}\left(c_\beta D^3_{3,4-j} - s_\beta D^3_{2,4-j}\right) \\ & - D^3_{1,4-j}\left(c_\beta D^3_{3,4-i} - s_\beta D^3_{2,4-i}\right). \end{aligned} \tag{81}$$

The Bose symmetry that forbids any anti-symmetric derivative coupling of a vector particle to two identical real scalar fields is respected, $g_{H_iH_iV} = 0$.

Finally the decay width of the H_i to SM fermions can be obtained from the decay width of the SM Higgs boson by multiplying it with

$$\left[\left(g^{\mathrm{S}}_{H_iff}\right)^2 + \left(g^{\mathrm{P}}_{H_iff}\right)^2\right], \tag{82}$$

with

$$g^{\mathrm{S}}_{H_iuu} = D^3_{3,4-i}/s_\beta, \quad g^{\mathrm{P}}_{H_iuu} = D^3_{1,4-i}\, c_\beta/s_\beta \tag{83}$$

$$g^{\mathrm{S}}_{H_idd} = D^3_{2,4-i}/c_\beta, \quad g^{\mathrm{P}}_{H_idd} = D^3_{1,4-i}\, s_\beta/c_\beta \tag{84}$$

for up- and down-type quarks respectively.

4.3 The special case of vanishing phases

In the $\mathcal{CP}$ conserving case, e.g. for the leading m_t^4 corrections $\phi_t = \phi_\mu = 0$, the $\mathcal{CP}$-even Higgs bosons (denoted as h and H with $m_h \leq m_H$) and $\mathcal{CP}$-odd Higgs boson (denoted as A) do not mix. The unrotated mass matrix is then given by

$$M_{\mathcal{CP}} = \tag{85}$$
$$\begin{pmatrix} \bar{M}^2_{H^\pm} - \hat{\Sigma}_{AA}(0) & 0 & 0 \\ 0 & m^2_{\phi_1} - \hat{\Sigma}_{\phi_1\phi_1}(0) & m^2_{\phi_1\phi_2} - \hat{\Sigma}_{\phi_1\phi_2}(0) \\ 0 & m^2_{\phi_1\phi_2} - \hat{\Sigma}_{\phi_1\phi_2}(0) & m^2_{\phi_2} - \hat{\Sigma}_{\phi_2\phi_2}(0) \end{pmatrix}$$

where the square of the $\mathcal{CP}$-odd Higgs boson mass is given by $M_A^2 = \bar{M}^2_{H^\pm} - \hat{\Sigma}_{AA}(0)$. For a large part of the MSSM parameter space the mass ordering for the three Higgs boson masses is given as $m_H \geq M_A \geq m_h$, i.e.

$$M^D_{\mathcal{CP}} = \begin{pmatrix} m_H^2 & 0 & 0 \\ 0 & M_A^2 & 0 \\ 0 & 0 & m_h^2 \end{pmatrix} \quad \text{and} \quad D^3 = \begin{pmatrix} 0 & 1 & 0 \\ s_\alpha & 0 & c_\alpha \\ c_\alpha & 0 & -s_\alpha \end{pmatrix}. \tag{86}$$

The mass ordering in (74) can thus imply that in the limit of vanishing phases H_2 is the $\mathcal{CP}$-odd Higgs boson.

5 Numerical examples and comparison with other approaches

The results obtained in Sect. 3.3, (56)–(67), have been compared analytically with the corresponding results presented in [13] (11)–(18c). Reference [13] calculates the leading corrections to the Higgs boson mass matrix in the EP approach. In the approximation of zero external momentum as applied in Sect. 3.3, the leading m_t^4 corrections as presented in (56)–(67) should therefore agree with the corresponding results in [13]. Differences due to different renormalization schemes are only expected from two-loop order on, see [7,9]. Complete analytical agreement between the two results is found, if the correction to $\mathcal{M}_H\Big|_{aa}$,the A boson propagator in (11) of [13] is identified with our renormalized A boson self-energy, $\hat{\Sigma}_{AA}$, given in (59). $\hat{\Sigma}_{AA}$ exhibits an additional term compared to the correction to $\mathcal{M}_H\Big|_{aa}$, arising from the fact that in [13] the charged Higgs boson sector has been neglected, while in our approach $M_{H^\pm}$ is chosen as an input parameter, thus introducing $\Sigma_{H^\pm}$ into the result. Therefore, this difference only reflects the fact of a different choice of input parameters. A similar observation has already been made in [13], while comparing with [14] (where also analytical agreement in the appropriate limits has been found.)

In the following subsections some numerical examples are presented and compared to results obtained in the RG improved EP calculation. The examples are based on the results given in Sects. 3.3, 3.4. They are meant to illustrate the possible effects of complex phases in the MSSM. For a phenomenological analysis, however constraints on $\mathcal{CP}$-violating parameters from experimental bounds on electric dipole moments (EDMs) have to be taken into account, see Sect. 6. On the other hand, the bounds from EDMs can easily be evaded by making the first two generations sufficiently heavy [24]. A more detailed phenomenological analysis of the FD results, including the full one-loop and leading two-loop corrections in the cMSSM to the Higgs boson self-energies, and taking into account all existing experimental constraints can be found in [17].

5.1 Higgs boson masses

In Fig. 3 the two lightest Higgs boson masses, m_{H_1} and m_{H_2}, are shown as a function of the phase of the trilinear coupling in the $\tilde{t}$ sector, φ_{A_t}. The soft SUSY-breaking parameters are chosen to emphasize the effect of the $\mathcal{CP}$-violating phases, $M_{SUSY} = 500\,\mathrm{GeV}$, $|A_t| = 1000\,\mathrm{GeV}$ and $|\mu| = 2000\,\mathrm{GeV}$. The phase of μ is chosen to be zero, except for the lower right plot, where it is set to $\varphi_\mu = \pi/2$. The phases in the b and τ sector are set to zero. The different plots show the variation with $\tan\beta$, $\tan\beta = 2, 5, 20$. In the $\mathcal{CP}$-conserving case for the above chosen soft SUSY-breaking parameters, $\tan\beta = 2$ is already excluded by Higgs boson searches [25]. However, in the $\mathcal{CP}$-violating case this limit is weakened [15] due to possible suppressed production cross section and/or suppressed decays of the lightest Higgs boson to b quarks, see Sect. 5.2. In each plot different values for the charged Higgs boson masses have been chosen, $M_{H^\pm} = 150, 200, 300, 500\,\mathrm{GeV}$. The largest effects of the phases are observed for small $\tan\beta$ and small $M_{H^\pm}$. For large $M_{H^\pm}$ the effects of the $\mathcal{CP}$-violating phases become negligible small.

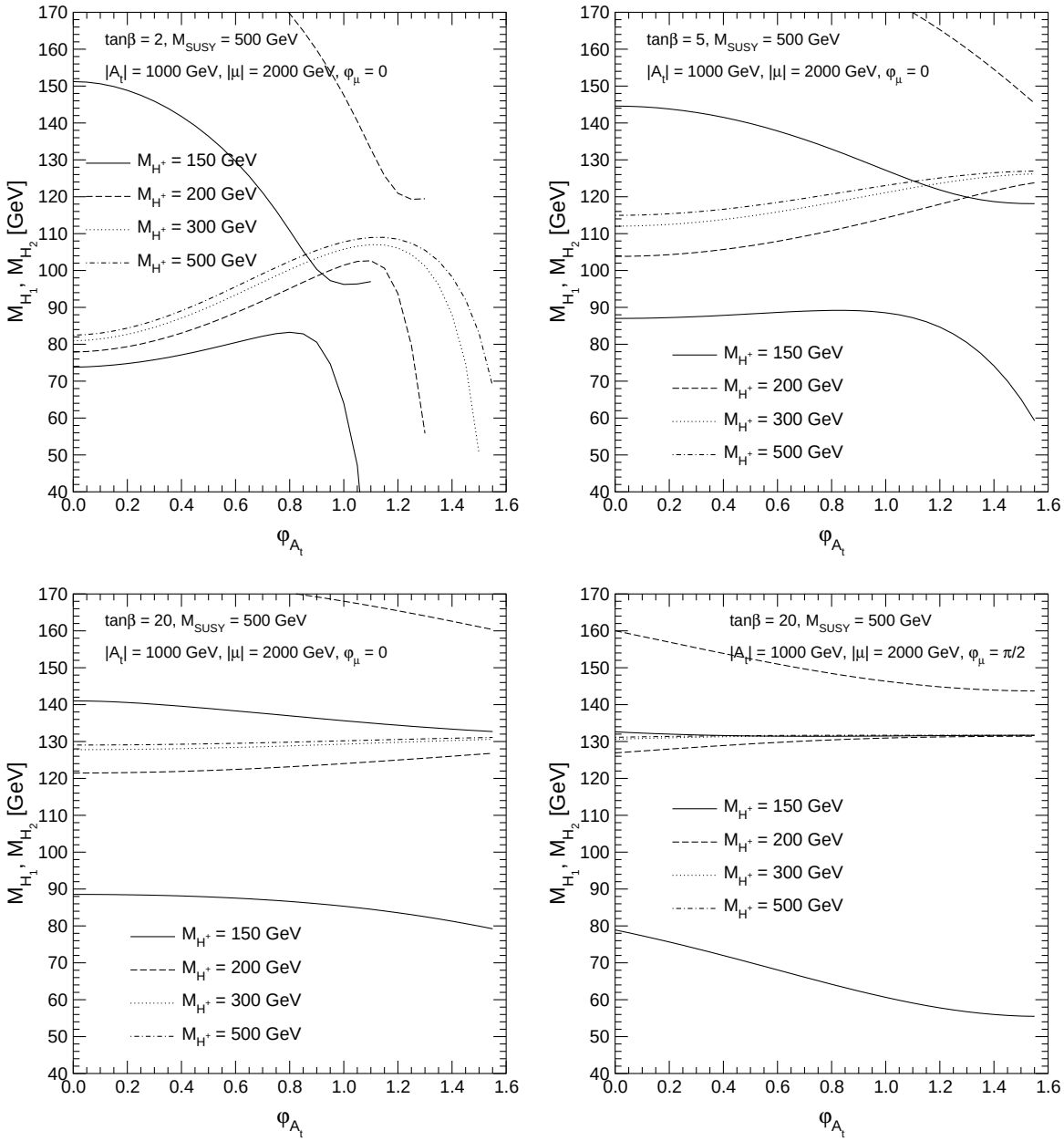

Fig. 3. The two lightest neutral Higgs boson masses are shown as a function of φ_{A_t} for different values of $M_{H^\pm}$. In the first three plots φ_μ is set to zero and $\tan\beta$ is chosen as $2, 5, 20$. In the last plot $\varphi_\mu = \pi/2$ and $\tan\beta = 20$ is taken. The other parameters are $M_{SUSY} = 500\,\text{GeV}$, $|A_t| = 1000\,\text{GeV}$ and $|\mu| = 2000\,\text{GeV}$

A numerical comparison with e.g. Figure 3 in [14] shows agreement better than 10% for not too large phases, $\phi_{A_t} \lesssim 0.8$. A larger phase corresponds to larger mixing in the t sector. This, on the one hand, makes the corrections and thus the uncertainties in the Higgs sector larger. On the other hand, the RG improved EP calculations tends to loose accuracy for too large mixing in the $\tilde{t}$ sector. The agreement improves slightly if a comparison with the more complete result of [15] (see e.g. Fig. 1) is performed. Furthermore, it has been shown in [7] that differences in the Higgs boson masses arising from different renormalizations can be significant, especially for large $\tilde{t}$ mixing. Therefore agreement better than 5-10% cannot yet be expected for all parameter sets due to the different renormalizations employed and the yet more complete evaluation performed in the RG improved EP calculation.

In Fig. 4 the mass difference of the two heavier Higgs bosons, $m_{H_3} - m_{H_2}$, is shown as a function of φ_{A_t}. The other parameters are chosen as in Fig. 3. A large enhancement of the mass difference can be observed for small $\tan\beta$. The agreement with [14,15] is found at the same level as for Fig. 3.

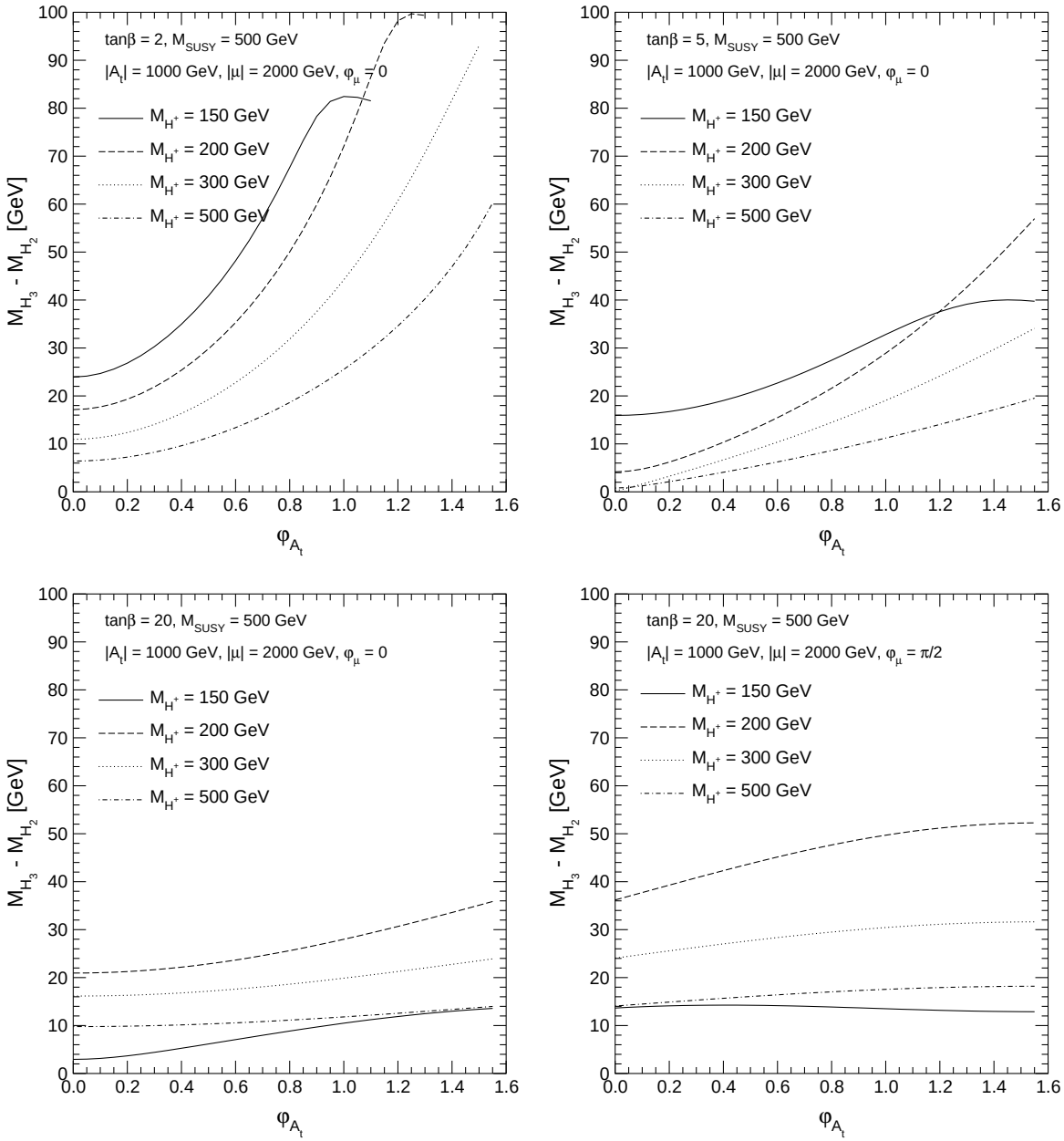

Fig. 4. The mass difference between the two heavy Higgs boson, $m_{H_3} - m_{H_2}$, is shown as a function of φ_{A_t} for different values of $M_{H^\pm}$. In the first three plots φ_μ is set to zero and $\tan\beta$ is chosen as $2, 5, 20$. In the last plot $\varphi_\mu = \pi/2$ and $\tan\beta = 20$ is taken. The other parameters are $M_{SUSY} = 500\,\text{GeV}$, $|A_t| = 1000\,\text{GeV}$ and $|\mu| = 2000\,\text{GeV}$

5.2 Higgs boson couplings

In Fig. 5 the coupling of the lightest Higgs boson to two SM gauge bosons, relative to its SM value, is shown as a function φ_{A_t}. The other parameters are chosen as in Fig. 3. Large suppressions occur for small values of $M_{H^\pm}$. For $M_{H^\pm} \gtrsim 250\,\text{GeV}$ no suppression could be observed. For small $\tan\beta$ the suppression can amount several orders of magnitude, whereas for large $\tan\beta$ a suppression by a factor of 10 can be observed. These results can be compared with the RG improved EP approach, [14] Fig. 5 and [15] Fig. 1. As for the Higgs boson masses, we find reasonable agreement for not too large values of ϕ_{A_t}.

In Fig. 6 the decay rate of the lightest Higgs boson to b quarks, $\Gamma(H_1 \to b\bar{b})$, relative to its SM value, is shown as a function φ_{A_t}. The other parameters are chosen as in Fig. 3. The MSSM decay rate, although dependent on the complex phases, is considerably larger than the SM one for most parts of the parameter space. This renders the $b\bar{b}$ channel the main decay channel also in the cMSSM.

6 The Fortran code *FeynHiggsFastC*

The results presented Sect. 3.3 and Sect. 3.4 are incorporated into the Fortran code *FeynHiggsFastC*. They are

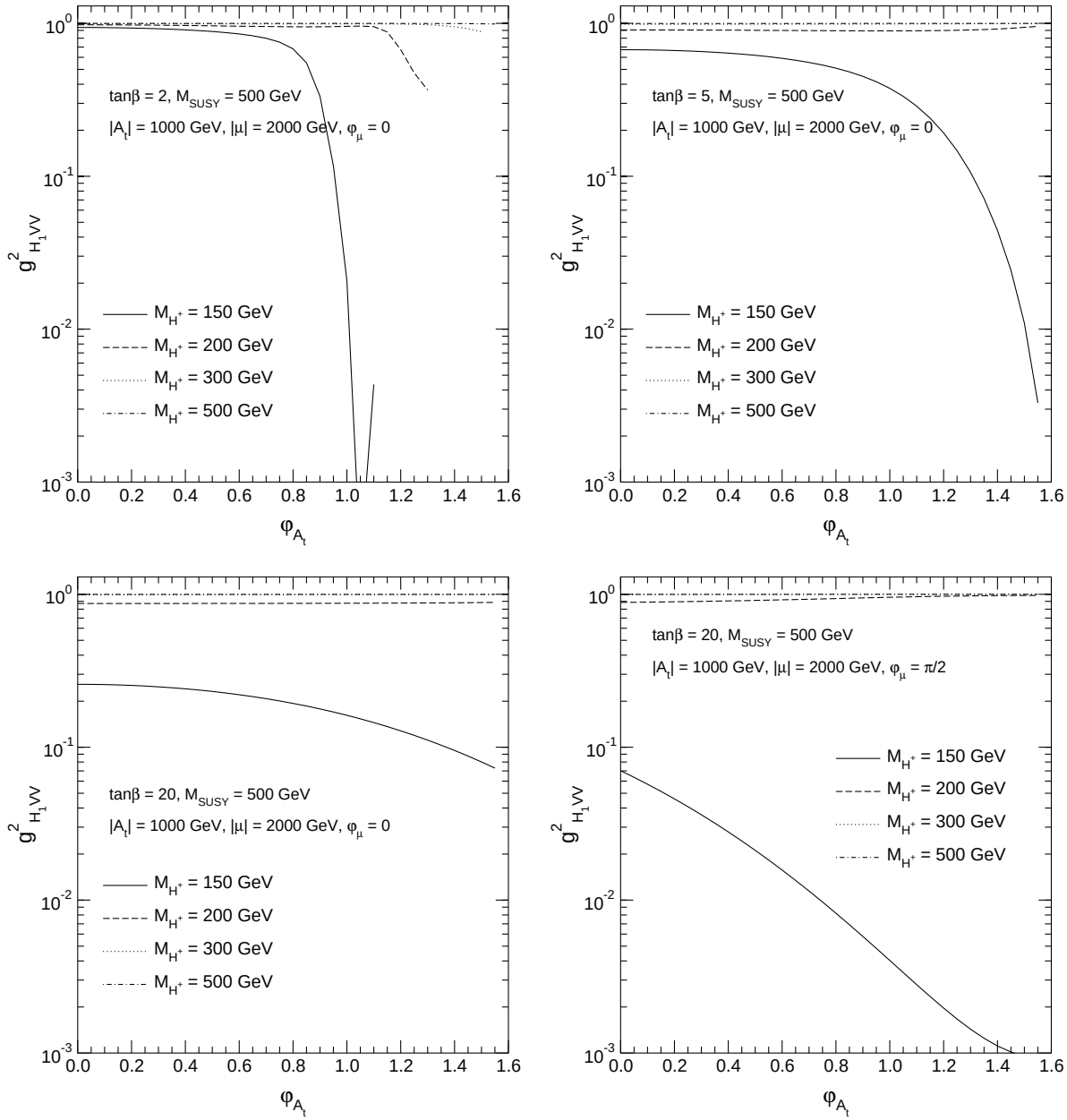

Fig. 5. The coupling of the lightest Higgs boson to two gauge bosons (relative to its SM value) is shown as a function of φ_{A_t} for different values of $M_{H^\pm}$. In the first three plots φ_μ is set to zero and $\tan\beta$ is chosen as $2, 5, 20$. In the last plot $\varphi_\mu = \pi/2$ and $\tan\beta = 20$ is taken. The other parameters are $M_{SUSY} = 500\,\text{GeV}$, $|A_t| = 1000\,\text{GeV}$ and $|\mu| = 2000\,\text{GeV}$

supplemented by the subleading one-loop corrections from the $t/\tilde{t}$ sector [22] as well as by the full logarithmic one-loop corrections from all other sectors of the MSSM, obtained in the RG approximation [4].

In the front-end of the code, the user can specify the input parameters, including all relevant complex phases. This part can be manipulated at the user's will. The main part of the code consists of the routines needed for the evaluation of the higher-order corrections to the neutral Higgs boson mass matrix, and should not be manipulated.

FeynHiggsFastC evaluates the following items in the cMSSM Higgs sector:

- the three neutral Higgs boson masses
- the effective couplings of one neutral Higgs boson to two SM gauge bosons and of two neutral Higgs bosons to a Z boson
- the changes in the branching ratio for a Higgs decaying to SM fermions

Furthermore the following "check items" are evaluated:

- the SUSY corrections to the ρ-parameter, coming from the $\tilde{t}/\tilde{b}$ sector. (The complex phases enter only via their effective change of the $\tilde{t}$ and $\tilde{b}$ masses, where they can enlarge the splitting and increase the contribution to

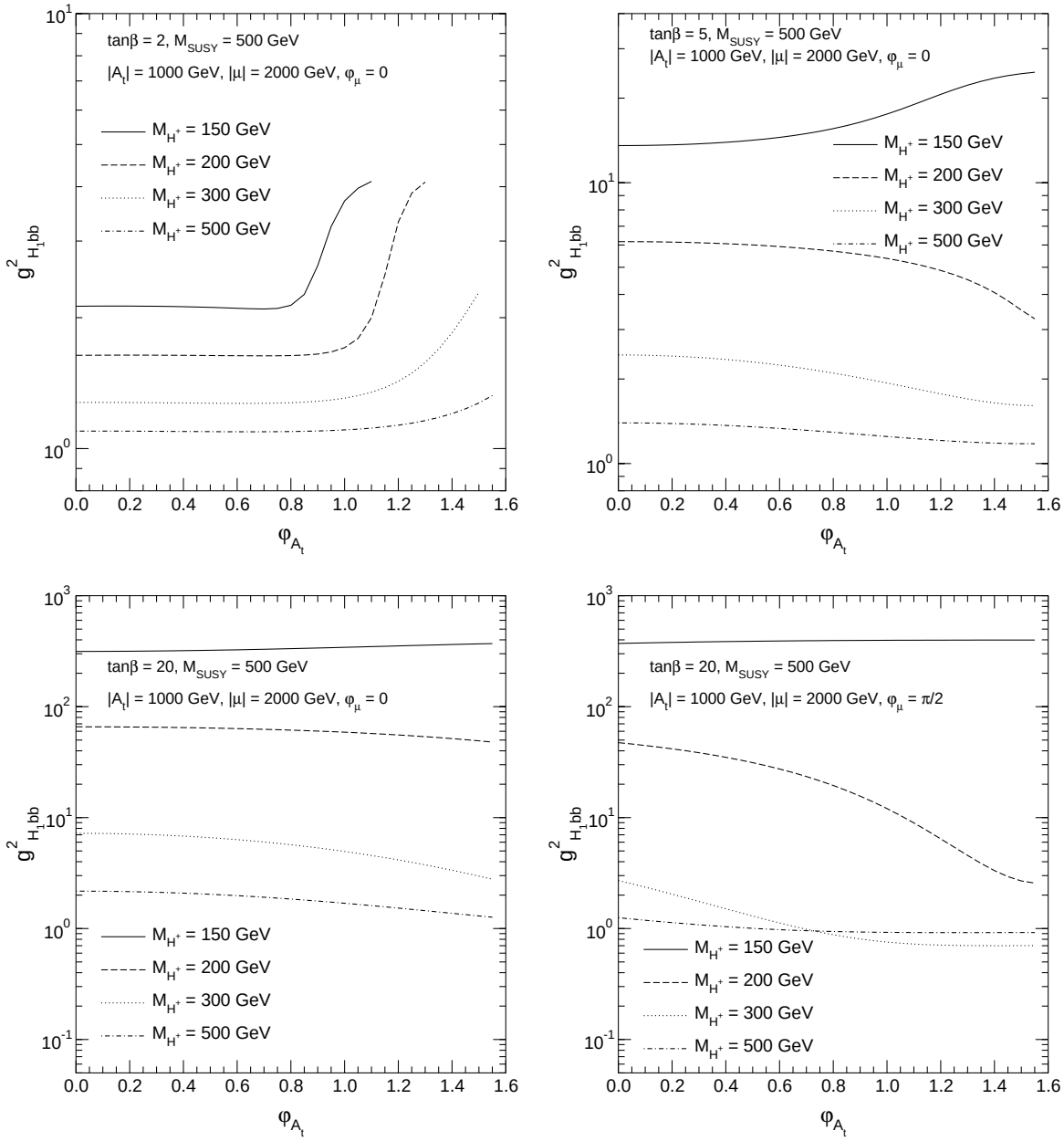

Fig. 6. The decay rate of the lightest Higgs boson to b quarks, $\Gamma(H_1 \to b\bar{b})$, relative to its SM value, is shown as a function of φ_{A_t} for different values of $M_{H^\pm}$. In the first three plots φ_μ is set to zero and $\tan\beta$ is chosen as $2, 5, 20$. In the last plot $\varphi_\mu = \pi/2$ and $\tan\beta = 20$ is taken. The other parameters are $M_{SUSY} = 500\,\text{GeV}$, $|A_t| = 1000\,\text{GeV}$ and $|\mu| = 2000\,\text{GeV}$

$\Delta\rho$.) The SUSY corrections are implemented in $\mathcal{O}(\alpha)$ and $\mathcal{O}(\alpha\alpha_s)$, where the gluino-exchange corrections, which go to zero for large $m_{\tilde{g}}$ have been omitted [26]. A value of $\Delta\rho$ outside the experimentally preferred region of $\Delta\rho^{\text{SUSY}} \lesssim 3 \times 10^{-3}$ [27] indicates experimentally disfavored $\tilde{t}$ and $\tilde{b}$ masses.

– the EDM of the electron and the neutron, following the calculation of [28][2] with the convention of common soft SUSY-breaking parameters for up- and down-type squarks. Values outside the experimentally allowed ranges indicate either too large $\mathcal{CP}$-violating phases or demand heavier squarks in the first two families [24].

The code can be obtained from the *FeynHiggs*[29] home page: `www.feynhiggs.de`.

7 Conclusions

We have presented the application of the Feynman-diagrammatic method and the on-shell renormalization scheme to radiative corrections in the Higgs sector of the

[2] We thank C. Schappacher for providing the corresponding Fortran code

MSSM with complex phases. This provides a complementary method to the (renormalization group improved) Effective Potential approach that has been used so far for phenomenological analyses. The presented set-up can then be used for a detailed study of the cMSSM Higgs sector in the FD/on-shell approach.

The general FD/on-shell method has been analyzed. Details about the renormalization in the on-shell scheme and the derivation of the renormalized Higgs boson self-energies have been presented. As an example the leading fermionic corrections to the cMSSM Higgs sector have been calculated analytically, making use of the recently completed MSSM model file for *FeynArts* 3. After showing the generic applicability of the approach, some numerical examples have been calculated. The leading fermionic corrections have been supplemented by the leading two-loop corrections. Results have been obtained for the masses of the neutral cMSSM Higgs bosons, their couplings to SM gauge bosons and their couplings to SM fermions. Reasonable agreement better than 10% with the RG improved EP method has been found for not too large mixing in the scalar top sector.

Finally the public Fortran code *FeynHiggsFastC* has been presented. It provides the evaluation of the masses and couplings of the cMSSM Higgs bosons in dependence of the relevant cMSSM parameters, including all possible complex phases. Besides the leading fermionic one-loop and the leading two-loop corrections, also the full logarithmic one-loop contributions, taken over from the real MSSM, have been implemented. The code is obtainable at `www.feynhiggs.de`.

Acknowledgements. We thank S. Dawson, M. Drees, A. Pilaftsis and C. Schappacher for helpful discussions and W. Hollik and C. Wagner for a critical reading of the manuscript. We furthermore thank T. Hahn, C. Schappacher and other members of the TP, Universität Karlsruhe, Germany, for their effort put into *FeynArts* and the new MSSM model file.

References

1. G. Kane, C. Kolda, J. Wells, Phys. Rev. Lett. **70**, 2686 (1993), hep-ph/9210242; J. Espinosa, M. Quirós, Phys. Rev. Lett. **81**, 516 (1998), hep-ph/9804235
2. J. A. Aguilar-Saavedra et al., TESLA TDR Part 3: "Physics at an e^+e^- Linear Collider", hep-ph/0106315, see: `tesla.desy.de`; T. Abe et al. [American Linear Collider Working Group Collaboration], "Linear collider physics resource book for Snowmass 2001", hep-ex/0106055, hep-ex/0106056, hep-ex/0106057, hep-ex/0106058
3. R. Hempfling, A. Hoang, Phys. Lett. B **331**, 99 (1994), hep-ph/9401219; R. Zhang, Phys. Lett. B **447**, 89 (1999), hep-ph/9808299; J. Espinosa, R. Zhang, Nucl. Phys. B **586**, 3 (2000), hep-ph/0003246
4. M. Carena, M. Quirós, C. Wagner, Nucl. Phys. B **461**, 407 (1996), hep-ph/9508343; H. Haber, R. Hempfling, A. Hoang, Z. Phys. C **75**, 539 (1997), hep-ph/9609331
5. S. Heinemeyer, W. Hollik, G. Weiglein, Phys. Rev. D **58**, 091701 (1998), hep-ph/9803277; Phys. Lett. B **440**, 296 (1998), hep-ph/9807423
6. S. Heinemeyer, W. Hollik, G. Weiglein, Eur. Phys. Jour. C **9**, 343 (1999), hep-ph/9812472
7. M. Carena, H. Haber, S. Heinemeyer, W. Hollik, C. Wagner, G. Weiglein, Nucl. Phys. B **580**, 29 (2000), hep-ph/0001002
8. S. Heinemeyer, W. Hollik, G. Weiglein, hep-ph/9910283
9. J. Espinosa, R. Zhang, JHEP **0003**, 026 (2000), hep-ph/9912236
10. G. Degrassi, P. Slavich, F. Zwirner, hep-ph/0105096
11. A. Pilaftsis, Phys. Rev. D **58**, 096010 (1998), hep-ph/9803297; A. Pilaftsis, Phys. Lett. B **435**, 88 (1998), hep-ph/9805373
12. D. Demir, Phys. Rev. D **60**, 055006 (1999), hep-ph/9901389
13. S. Choi, M. Drees, J. Lee, Phys. Lett. B **481**, 57 (2000), hep-ph/0002287
14. A. Pilaftsis, C. Wagner, Nucl. Phys. B **553**, 3 (1999), hep-ph/9902371
15. M. Carena, J. Ellis, A. Pilaftsis, C. Wagner, Nucl. Phys. B **586**, 92 (2000), hep-ph/0003180
16. A. Dabelstein, Nucl. Phys. B **456**, 25 (1995), hep-ph/9503443; Z. Phys. C **67**, 495 (1995), hep-ph/9409375; P. Chankowski, S. Pokorski, J. Rosiek, Nucl. Phys. B **423**, 437 (1994), hep-ph/9303309
17. M. Frank, S. Heinemeyer, W. Hollik, C. Schappacher, G. Weiglein, in preparation
18. J. Gunion, H. Haber, G. Kane, S. Dawson, The Higgs Hunter's Guide, Addison-Wesley, 1990
19. J. Küblbeck, M. Böhm, A. Denner, Comp. Phys. Comm. **60**, 165 (1990); T. Hahn, Nucl. Phys. Proc. Suppl. **89**, 231 (2000), hep-ph/0005029; hep-ph/0012260. The program and the user's guide is available via `www.feynarts.de`
20. T. Hahn, C. Schappacher, hep-ph/0105349
21. See user's guide in [19]; see also: S. Heinemeyer, BNL–HET–00/48, hep-ph/0102318, to appear in the proceedings of the ACAT2000, Fermilab, Oct. 2000
22. S. Heinemeyer, W. Hollik, G. Weiglein, Phys. Lett. B **455**, 179 (1999), hep-ph/9903404
23. M. Carena, P. Chankowski, S. Pokorski, C. Wagner, Phys. Lett. B **441**, 205 (1998), hep-ph/9805349
24. P. Nath, Phys. Rev. Lett. **66**, 2565 (1991); Y. Kizukuri, N. Oshimo, Phys. Rev. D **46**, 3025 (1992)
25. LEP Higgs Working Group Collaboration, hep-ex/0107030; S. Heinemeyer, W. Hollik, G. Weiglein, JHEP **0006**, 009 (2000), hep-ph/9909540
26. A. Djouadi, P. Gambino, S. Heinemeyer, W. Hollik, C. Jünger, G. Weiglein, Phys. Rev. Lett. **78**, 3626 (1997), hep-ph/9612363; Phys. Rev. D **57**, 4179 (1998), hep-ph/9710438; S. Heinemeyer, G. Weiglein, hep-ph/0102317
27. Part. Data Group, Eur. Phys. Jour. C **15**, 1 (2000)
28. S. Pokorski, J. Rosiek, A. Savoy, Nucl. Phys. B **570**, 81 (2000), hep-ph/9906206
29. S. Heinemeyer, W. Hollik, G. Weiglein, Comp. Phys. Comm. **124** 2000 76, hep-ph/9812320; hep-ph/0002213. The codes are accessible via `www.feynhiggs.de`